

Received March 31, 2021, accepted April 10, 2021, date of publication April 16, 2021, date of current version April 28, 2021.

Digital Object Identifier 10.1109/ACCESS.2021.3073574

# Dynamic Wavelength Grouping for Quality of Service in Optical Packet Switching

HAFSA BIBI<sup>1</sup>, FARRUKH ZEESHAN KHAN<sup>1</sup>, MUNEER AHMAD<sup>2</sup>, (Member, IEEE),  
ANUM NASEEM<sup>1,3</sup>, TOMASZ HOLYSKI<sup>4</sup>, KELVIN J. A. OOI<sup>5</sup>, AND JAVED AHMED MAHAR<sup>6</sup>

<sup>1</sup>Department of Computer Science, University of Engineering and Technology, Taxila, Taxila 47050, Pakistan

<sup>2</sup>Department of Information Systems, Faculty of Computer Science and Information Technology, Universiti Malaya, Malaya 50603, Malaysia

<sup>3</sup>Department of Computer Science and Information Technology, The University of Lahore, Islamabad 44000, Pakistan

<sup>4</sup>Institute of Statistics and Mathematical Methods in Economics, Vienna University of Technology, 1040 Vienna, Austria

<sup>5</sup>Department of Physics, Xiamen University Malaysia, Sepang 43900, Malaysia

<sup>6</sup>Department of Computer Science, Shah Abdul Latif University, Khairpur 66020, Pakistan

Corresponding authors: Farrukh Zeeshan Khan (farrukh.zeeshan@uettaxila.edu.pk), Muneer Ahmad (mmalik@um.edu.my), and Kelvin J. A. Ooi (kelvin.ooi@xmu.edu.my)

This work was supported by the Xiamen University Malaysia under Project XMUMRF/2019-C3/IECE/0003.

**ABSTRACT** This paper concerns Quality of Service (QoS) provisioning in Optical Packet Switching (OPS) networks. We address the topic by proposing Dynamic Wavelength Grouping (DWG) for OPS, in this technique, available wavelengths are dynamically partitioned and allocated at each network link to particular classes of service. DWG adapts to traffic fluctuations by tracking the load status of every class of traffic and then schedules optical packets over group of wavelengths assigned for each class of service. Performance is examined using an own developed simulator. This simulator models various aspects of OPS in far detail. Two network topologies are studied under various parameter settings and traffic scenarios. DWG clearly outperforms its earlier static counterpart (SWG). It appears as flexible approach, efficiently functional even when the share of the high-priority load is temporarily low. Consequently, it minimizes the total blocking probability while preserving the desired service differentiation. We report also significant improvements in the network throughput.

**INDEX TERMS** Dynamic wavelength grouping (DWG), network simulation, optical packet switching, quality of service.

## I. INTRODUCTION

Transmission networks of today carry enormous and exponentially growing amounts of traffic, produced by multimedia, file download, and variety of interactive applications. In their backbone section, these networks rely greatly on Wavelength Division Multiplexing (WDM) and architectures tending towards nearly all-optical solutions. The underlying switching mechanisms can be categorized roughly in three groups: Optical Circuit Switching (OCS), Optical Packet Switching (OPS) and Optical Burst Switching (OBS).

In OCS, the network is configured in a way that wavelengths (circuits) are dedicated to single connections of higher-level clients from an ingress to an egress node, for relatively long periods of time. The nature of OCS is quasi-static, there are no packet drops and there is no jitter, but in presence of fluctuating demands, the utilization of resources may be

completely inefficient. Quite opposite in terms of switching granularity is OPS [1], [2]. It follows hop-by-hop transmission of optical packets comprising multiple higher-level client packets. The optical packets are assembled at the edge nodes electronically but their buffering and routing at the core nodes should be performed exclusively in optical layer. Thus, OPS provides much higher utilization, flexibility and scalability at the expense of technological advancements of optical components. In its basic version, of course OPS has higher Packet Delay Variation (PDV), Packet Loss Ratio (PLR) and transmission delay than OCS. However, today's applications and bursty nature of traffic streams clearly require the highly dynamic connectivity offered by OPS.

Finally, OBS is a compromise between the two above-mentioned paradigms [3]. Here, higher-level packets are also assembled at the edge (into relatively large 'bursts') but traverse the core nodes all-optically, i.e., without any buffering and processing. To resolve contention at the core nodes, for each burst an out-of-band control packet is sent

The associate editor coordinating the review of this manuscript and approving it for publication was P. Venkata Krishna<sup>1</sup>.

ahead to configure cross-connects along the transmission path precisely for the time of burst transmission. OBS attracted a lot of attention and multiple variants have been proposed in literature. Nevertheless, OBS presents some technological challenges too. One of them is implementation of Fiber Delay Lines (FDLs) to delay the particular bursts when contention resolution is needed. Also, performance evaluation of OBS is quite complicated to evaluate. In literature, different mathematical models and simulation studies has been presented under very different network of settings and model assumptions; compare e.g., [4]–[8]. Global conclusions based on analysis of selected mechanisms of OBS are therefore very difficult.

The main difficulty related with OPS is of course the need of all-optical header processing. Therefore, the current feasible and more realistic version of OPS assumes separation of header and payload at each traverse node. The header undergoes Optical-Electrical-Optical (OEO) conversion and is electronically processed for routing and scheduling purpose. The payload stays in optical domain and is buffered (delayed) by means of FDLs [9]. Even in this limited version, OPS is perceived as highly attractive. First and the foremost, it provides energy efficient communication. Considerable power savings are possible due to absence of bit-by-bit OEO conversions of the payloads. Secondly, transmission rates are not limited to rates of electronic line cards, as it is the case of the traditional packet switching routers working fully in store-and-forward manner.

The highly random nature of optical packet traffic (more random than that of OBS network traffic) necessitates efficient Quality of Service (QoS) solutions to support different traffic classes and meet needs of versatile end-user applications. As widely known, multimedia applications require precise real-time provisioning. In particular, video streaming and online gaming pose high requirements on delay and jitter. In contrast, file download requires more throughput but accepts larger delays, and jitter is not a crucial factor. It is anticipated that newly emerging applications like data-center interconnection, tele-surgery or 3-dimensional television may pose even higher and/or more complex QoS demands; see [10], [11].

The main concern with QoS in OPS is that traditional solutions of IP networks do not carry over to OPS directly because of absence of the store-and-forward functionality. Therefore, recent years witnessed an intensive debate on QoS, dedicated specially to OPS. In fact, there is a multitude of related proposals since QoS can be implemented at various “instances” of OPS. One distinguishes QoS implemented in (or supported by) packet aggregation, wavelength reservation, packet dropping or access limitation. These schemes quite divide into the pro-active [12] and the reactive ones [13].

In this research work, we propose a novel QoS approach categorized as Dynamic Wavelength Grouping for OPS (DWG-OPS). We would point out that the static wavelength grouping, and its impact on overall performance of OBS networks have already been considered in [14]. However,

there remains some constraints in static wavelength grouping, if traffic share of High Priority (HP) traffic is very less as compared to total traffic, the static wavelengths assigned to HP traffic remain underutilized. Therefore, the total blocking probability increases resulting less throughput of the network. This fact is established in our previous work [14]. The solution to this problem is to group wavelengths dynamically according to incoming traffic load. Presently, in the context of OPS, we put forward a fully dynamic distribution of wavelengths to provide satisfactory QoS performance for different classes of traffic. Our precise objective is to analyze changes in packet blocking probabilities and network throughput resulting from particular partitioning of wavelengths among the classes. This analysis is based on simulations for two well-known network topologies, NSFNet and Cost239. Following are the contributions of this research work:

- Designed and analyzed a novel QoS technique “DWG-OPS”.
- Successfully achieved QoS in OPS networks.
- Total blocking probability is reduced on varying load scenarios.
- Network throughput is increased significantly.

The rest of the paper is organized as follows. Section II introduces the notion of QoS, explains the QoS requirements in OPS networks and gives overview of the techniques proposed in literature by now. Section III describes the baseline OPS network model that is assumed in this work. Section IV describes functioning of the proposed technique, the DWG-OPS, in more detail. Our simulation-based implementation is described in section V whereas discussion of experimental results and evaluation of the proposal is given in Section VI. Finally, Section VII concludes the whole work.

## II. QUALITY OF SERVICE (QoS) IN OPS NETWORKS

QoS refers to the potential of a network to deliver improved services to particular traffic classes. It includes management of resources and traffic control to provide performance differentiation among service providers or end users in order to meet requirements of their specific obligations and applications [15]. QoS for the end users concerns, in first place, the reception of the quality of an individual service out of the network with guarantee of performance metrics such as minimum delay, improved PLR or blocking probability, bandwidth assurance and limited jitter. In turn, QoS for a network means an efficient utilization of network resources for best-effort services.

On the other hand, two modes of QoS can be distinguished: absolute and relative. In relative QoS, the performance of individual class is determined relatively in comparison with other classes, and not explicitly defined in absolute terms. For instance, assuming High Priority (HP) and Low Priority (LP), the HP traffic definitely experiences a lower blocking probability than LP. Still, blocking of HP can be influenced by the traffic share of the LP class, and there is no guaranteed upper bound on that blocking probability for the HP class.

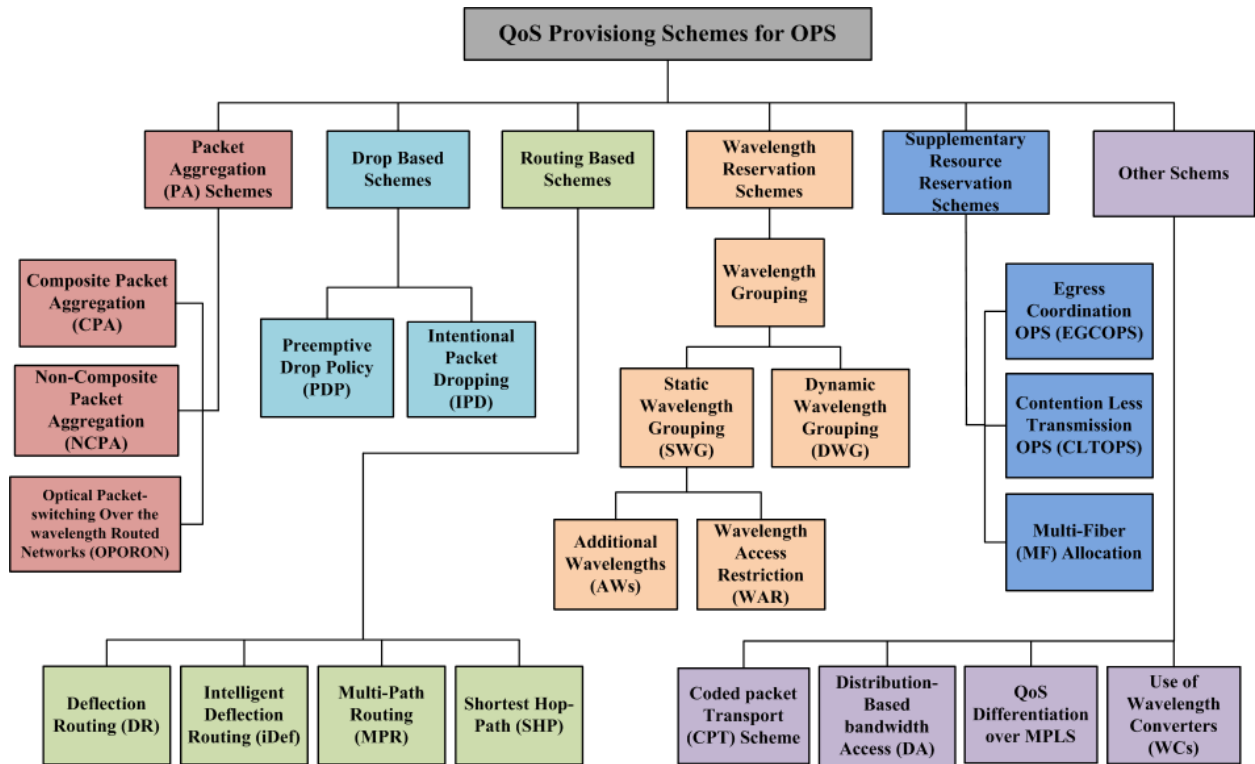


FIGURE 1. Different QoS Schemes for OPS Networks.

In contrast, there is an upper bound for blocking probability of guaranteed traffic (fixed total load of HP traffic) in the absolute QoS mode. This means that HP blocking probability does not depend at the existent share of the lower classes. This kind of rigid guarantee is feasible in multimedia and mission-critical applications so that these applications would be supported in other constraints like less delay and more bandwidth. However, efficient resource provisioning and admission control mechanisms are required to support the QoS in the absolute mode [16].

Provisioning of good QoS is essential for successful development of the next-generation optical packet networks with exponentially growing number of users that generate heterogeneous traffic streams [17]. Clearly, a QoS-aware OPS backbone is needed to handle the dynamic loads at core links for different classes of traffic. The relevant parameters and QoS-related quantities are, among others, PLR, blocking probability, error rate, delay, bandwidth, recovery time, fault tolerance, availability, reliability, response time and throughput [18]. In particular, lowering the PLR and blocking probability of HP packets is the main concern [19].

The approaches to QoS in OPS proposed till now in literature can be grouped into the following schemes:

- *packet aggregation schemes* [20] such as Composite Packet Aggregation and Non-Composite Packet Aggregation (CPA and NCPA), and Optical Packet-switching Over wavelength Routed Networks (OPORON) [21];

- *wavelength reservation schemes*: Additional Wavelengths (AWs) for the same traffic [22] and Wavelength Access Restriction (WAR) [23];
- *supplementary resource reservation*: Egress Coordination OPS (EGCOPS) [24], Contention Less Transmission OPS (CLTOPS) [25] and Multi-Fiber (MF) Allocation [26];
- *drop-based schemes*: Intentional Packet Dropping (IPD) [28], and Preemptive Drop Policy (PDP) [28];
- *routing-based schemes*: Deflection Routing (DR) [29], Intelligent Deflection Routing (iDef) [30], Multi-Path Routing (MPR) [29] and Shortest Hop-Path (SHP) [31];
- *access limitation*: FDL-access limitation [32] and Distribution-based bandwidth Access (DA) [33];
- *other schemes and solutions*: Coded Packet Transport (CPT) Scheme [27], QoS Differentiation over MPLS [34], use of Wavelength Converters (WCs) [35].

The taxonomy of the schemes is depicted in Fig. 1 whereas their good overview is given by [1]. Performance analyses of selected schemes are presented, for example, in [36] and [35], [37], [38].

In what follows, we focus on QoS through wavelength grouping, which is associated with a quite fine group of schemes that assure absolute QoS, i.e., wavelength reservation schemes. In this scheme, a group of wavelengths is allocated to different priorities of traffic. Traditionally, wavelength assignment is fixed so it is termed as Static Wavelength Grouping (SWG). All the wavelengths are distributed into disjoint wavelength subgroups and one subgroup is dedicated

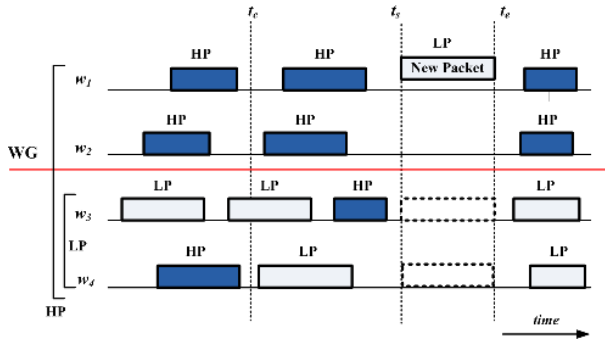


**FIGURE 2.** Scheduling through Static Wavelength Grouping with Four Wavelengths.

exclusively for only one priority traffic [14], [39]. Here, QoS is realized with unfair partitioning of available wavelengths. Also, priority classes do not compete for the resources, illustrated in Fig. 2.

More specifically, Wavelength Access Restriction (WAR) techniques restrict the access of LP packets to the OPS network resources in order to ensure an elevated link capacity for HP optical packets as compared to LP ones. This restriction causes a negative impact on the LP optical packets as they experience higher delays and congestion than that of HP ones. Moreover, resource reservation for a particular traffic class leads to the inefficient employment of network resources. This is possibly the main drawback of the WAR techniques. Additional Wavelengths (AWs), on the other hand, consumes extra wavelength resources to transmit the same traffic on each connection link in order to reduce blocking for HP optical packets. Use of AWs results in high network cost, as it requires more transceivers in ingress and egress switches for operation. The position of wavelength grouping among other prominent QoS schemes can be seen in Fig. 1.

Although wavelength grouping is more advanced and advantageous technique as compared to other QoS techniques but there are some issues in its static version. For example, with change in traffic loads of HP and LP, HP packets may occupy all the wavelengths which may increase drop rate for LP packets. In a scenario where traffic has less share of HP packets, there is significant possibility of under utilization of network resources. Also, this technique is less efficient in fluctuating traffic loads and arrival rates which result in an increased overall packet dropping. These problems effect the performance of network in sense of low throughput and higher delays. So, there is need of a more flexible approach which can overcome these limitations.

### III. BASELINE OPS NETWORK MODEL

In our model, we considered an asynchronous OPS backbone network comprising many wavelength-selective cross-connect optical switches. Each active switch is referred as a core switch and it is assumed that there are no passive switches. A particular core switch is possibly connected to one or more edge nodes and to multiple other core switches by  $n$  input and  $n$  output links. An individual link contains

multiple optical fibers whose number is denoted by  $f$ . In turn, each single fiber holds  $w$  wavelength channels. On the other hand, in the multifiber scenario, one input/output link is composed of  $f$  input/output ports.

Together, there are  $n_k + 1$  edge nodes with electronic buffers and  $n_k + 1$  core switches. Fig. 3 illustrates the intended node architecture in the data plane. The wavelength channels are available in the core switches by  $n \times n$  precisely non-blocking switches. Each core switch is connected to not more than  $n_k - 1$  core switches (core switches can send and receive data at the same time) and one ingress and one egress switch (these can be referred also to as the source and destination nodes, respectively). Through an ingress node  $n_k$  flows are injected into the network, and these flows are directed to  $n_k$  different egress nodes. Each output-link fiber holds  $w$  wavelengths for carrying data with rate  $B$  bit/s and one supplementary wavelength carrying control information.

It is assumed that the network carries  $\Psi$  priority classes of traffic, where each class is distinguished on the basis of required QoS traits. An ingress node can send data up to  $w_{ci}$  optical packets simultaneously at the beginning of each time-slot. A time-slot comprises of  $w_{ci}$  optical packets is referred to as an optical slot. Such slot remains unused until arrival of an optical packet. Each optical packet contains an integer number of IP packets with same destination and QoS class, however, its size may vary.

Each optical packet consists of a control information (termed optical header), a trivial guard time-band and payload data. Information about source or destination, packet type and priority are contained in the optical header. The transmission time (size in time) the optical header and the guard time-band are denoted as  $t_G$  and payload's transmission is  $t_{P\Psi}$ . Therefore, duration of a time slot  $t_{slot}$  is expressed as  $t_{slot} = t_{P\Psi} + t_G$ .

An ingress node has  $n_k$  electronic buffers, called assembly queues, that hold arriving IP packets with the same destination (the same address of the egress switch). IP packets incoming to the egress switch are assembled into optical packets in the assembly queues on the hybrid time-length basis. In this approach, packets are assembled until either a fixed maximum aggregation timer  $T_{aggr}$  of the buffer expires or total size of the aggregated packets plus a newly arrived IP packet exceeds certain length of  $P_{size}$  bits ( $P_{size} = t_{P\Psi} \times B = t_e - t_s$ , where  $t_s$  is start time and  $t_e$  is end time). Value of  $T_{aggr}$  is chosen so the IP packets should not wait too long at the assembly queues if packet arrival streams are not intense. The same refers to the choice of  $P_{size}$ . Trade-offs between  $T_{aggr}$  and  $P_{size}$  have been studied in literature in context of OPS, see e.g., [6].

After the assembly, all IP packets of the assembly queues are aggregated into an optical packet and forwarded to the electronic dispatch buffer with First Come First Serve (FCFS) queueing strategy. There, the aggregated packets are sent towards the scheduling module, passing first the routing module [40]. A flow  $n_k$  at an ingress node includes all optical packets which are moved from an ingress node to an



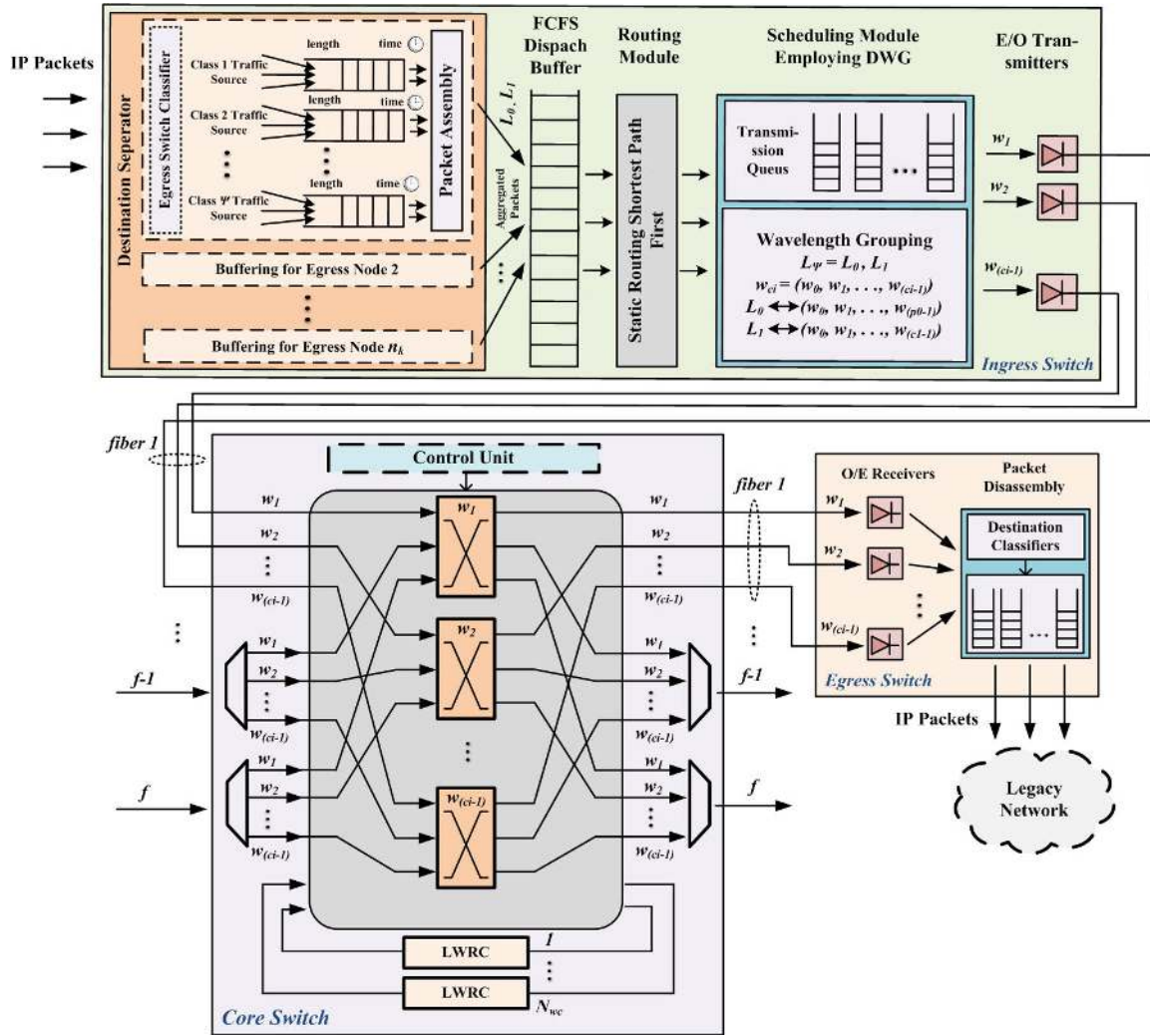


FIGURE 3. Data Plane Architecture of Baseline OPS Node.

egress node  $n_k$ . A flow contains IP packets from multiple connections and multiple applications which come in the same ingress node and go out from the corresponding egress node and passes through the comparable paths in the optical network.

Static routing is there in routing module for selection of best routing path on the basis of shortest path. Input and output fibers with wavelengths at a switch are combinedly called out as input/output port at that switch [41], [42]. Accordingly, in a network where there is  $n_k$  egress nodes and  $\Psi$  service classes, each ingress node keeps  $n_k \Psi$  buffers. The scheduler transmits the optical packets to the network on the available wavelengths or fibers. To control the service order of IP packets from different sources, dedicated buffers are used for the traffic of each individual source router. The cooperative interconnections of all these components in the OPS node can be realized in Fig. 3.

Payload of incoming optical packets of all input interfaces at a core switch waits in FDLs until header is processed and a new header is generated according to the control information so that core switch may switch non-contending

optical packets to an output port. Amongst remaining contending optical packets for the same output port, the core switch selects an optical packet at random and transmits it on the requested output fiber at a different unused wavelength using a Limited-Range Wavelength Converters (LRWC), until all the contending optical packets get examined or all the LRWCs get utilized. The optical packets which are unable to be sent even by means of LRWC, are dropped. There is no retransmission pattern in our baseline OPS network model, retransmissions can also be added in the optical domains to buffer-less OPS networks [43].

#### IV. DYNAMIC WAVELENGTH GROUPING FOR QoS IN OPS

As already explained briefly that in static version of wavelength grouping [14], [39], the wavelength assignment is predefined and fixed. Each disjoint subgroup of wavelength is reserved entirely for one priority class so there is no competition for wavelength resources. However, from network performance perspective, it is revealed that this uncompromising behavior of SWG is inefficient in fluctuating traffic loads (varying share of HP and LP traffic in total load) and

arrival rates which results in higher blockings of traffic and therefore overall low throughput [14].

These limitations let us devise a more refined approach named “Dynamic Wavelength Grouping (DWG)” as a solution for the stated problems of SWG. In dynamic variant of wavelength grouping, every wavelength is allowed to carry optical packets of any priority class until the total number of occupied wavelengths for that priority is less than some fixed limit. Furthermore, an optical packet of the highest priority class may occupy all the available wavelengths which possibly will reduce the packet losses of output port contentions.

Since our baseline reference OPS network is operative on static routing and has no deflection routing, so apparently optical packets of the same source address and destination address will pass through the same routes and will face same end-to-end delay measure in the OPS network. The DWG is applied at all switching nodes at OPS network. In brief, DWG works in the following way. The packets received at an ingress node from legacy network are IP packets or client packets, for QoS differentiation, IP packets of different classes (based on their priority) are assembled to form optical packets of respective priorities.

For each priority class  $\Psi$  of traffic, there is an assembly queue for every destination where IP packets are assembled on the basis of time-length hybrid assembly, defined in previous section. Each newly generated optical packet is sent over routing module to FCFS dispatch buffer, where it stays and waits up until scheduling module determines best wavelength for transmission. The priority-based classification of the traffic assists each service class to use a provisioned set of wavelengths by assigning a unique identification label to each class. In general, class  $\Psi$  traffic is labeled with  $L_\Psi$ , and a set of wavelengths  $w_{pi}$  out of the total available wavelengths  $w_{ci}$  at each link  $l$ . In other words, a link  $l$  must surely make available at least  $w_{pi}$  wavelengths for optical packets of label  $L_\Psi$ .

$$L_\Psi = \left( \frac{\sum_{i=1}^n t_{p\Psi} \times B}{t_c} \right) / w_{ci} \quad (1)$$

In our work, we considered a network having traffic from two classes, where  $\Psi$  for HP traffic is 1 and  $\Psi$  for LP traffic is 0. As HP traffic is represented by class 1 and so, a HP optical packet is assigned with label  $L_1$ , while LP traffic is represented by class 0 and hence, a LP optical packet is assigned with label  $L_0$ . Current load on a link  $l$  is obtained from Eq. 1, where  $t_{p\Psi}$  is packet size of a packet either HP or LP,  $B$  is data rate,  $t_c$  is current time and  $w_{ci}$  are total wavelengths on a link  $l$ .

$$T(L_0, L_1) = \begin{cases} \left( \frac{\sum_{i=1}^n t_{p0} \times B}{t_c} \right) / w_{ci} & \text{if } L_\Psi = L_0 \\ \left( \frac{\sum_{i=1}^n t_{p1} \times B}{t_c} \right) / w_{ci} & \text{if } L_\Psi = L_1 \end{cases} \quad (2)$$

Share of one class of traffic  $T(L_0, L_1)$  with a given label  $L_\Psi$ , calculated from the total load value of Eq. 1, is determined by Eq. 2. Here  $L_0$  and  $L_1$  contribute to make total load

on a  $l$  at current time  $t_c$ .  $T(L_0, L_1)$  gives the load value of HP and LP packets separately in order to find out the exact share of each priority class. In other words, we can write  $T(L_0, L_1)$  as a sum of  $L_0$  and  $L_1$ .

Then Eq. 3, gives the percentage  $\eta$  of that class in current total load on a link  $l$ . In our example, for  $L_0$ , it is assumed that if share of  $L_1$  goes to 0,  $L_0$  will constitute the maximum share in total load and  $\eta$  of  $L_\Psi$  can be taken as  $\eta$  of  $L_0$  solely, otherwise it is acquired from  $L_0/L_\Psi$ .

$$\eta = \begin{cases} L_\Psi & \text{if } L_1 \rightarrow 0 \\ \frac{L_0}{L_\Psi} & \text{otherwise} \end{cases} \quad (3)$$

Number of wavelengths  $w_{p0}$  required for carrying  $\eta$  of  $L_\Psi$  is determined directly from Eq. 4 by simply multiplying the  $\eta$  with  $w_{ci}$  in current  $l$ , and a set of  $w_{pi}$  wavelengths is provisioned from Eq. 5. If  $w_{p0}$  wavelengths on current link  $l$  are needed to transmit  $L_0$  optical packets, then a first  $w_{p0} = (w_0, w_1, \dots, w_{p0-1})$  wavelengths from  $w_{ci}$  are reserved for  $L_0$  optical packets where  $w_{p0} < w_{c1}$ . In this way,  $L_0$  optical packets can only use wavelengths from this reserved set of wavelengths. HP packets ( $\eta$  for  $L_1$ ) are allowed to be scheduled on any wavelengths  $w_{p1} = (w_0, w_1, \dots, w_{p1-1})$  from total  $w_{ci}$  where  $w_{p1}$  can reach up to all  $w_{ci}$  of  $l$ .

$$w_{pi} = \eta \times w_{ci} \quad (4)$$

$$w_{pi} = \begin{cases} w_{p0} = \sum_{ci=1}^{p0-1} w_{ci} & \text{where } w_{p0} < w_{c1} \\ w_{p1} = \sum_{ci=1}^{p1-1} w_{ci} & \text{where } w_{p1} \leq w_{c1} \end{cases} \quad (5)$$

An optical packet can be scheduled dynamically on any usable wavelength if there is enough lengthy void to hold the newly incoming optical packet and number of occupied wavelengths of  $L_0$  optical packets are still less than the  $w_{c1}$ . This way, optical packets of the highest priority ( $L_1$  optical packets in our example) may take up  $w_{c1}$  wavelengths depending upon the share of highest priority traffic. Note that, a scheduling module also controls the switching matrix that manages the transit packets contending with the local packets, for availing the wavelengths. Switching nodes keep track of total number of wavelengths occupied by  $L_0$  optical packets so that number of engaged wavelengths do not exceed the provisioned number  $w_{p0}$ . This is necessary to prevent other classes of traffic from being suppressed, and to keep network consistently QoS-qualified regardless the varying share of both the classes in total load.

Fig. 4 shows the functioning of DWG in two service class traffic and four wavelengths scenario. Initially, it is assumed that two wavelengths are available for the  $L_0$  class while  $L_1$  can access all the four wavelengths. When  $L_0$  optical packet arrives at time  $t_c$ ,  $w_3$  and  $w_4$  are only available for scheduling of  $L_0$  with latest available unscheduled time [14], [39]. But when  $T(L_0, L_1)$  changes over time,  $w_1$  and  $w_2$  can also be reserved for  $L_0$  depending upon  $\eta$ . A concrete scheduling approach, Composite Edge-Core Scheduling with Void Filling (CECS-VF) [44] is used for scheduling of packets along with DWG, whose implementation can be understood in [44].

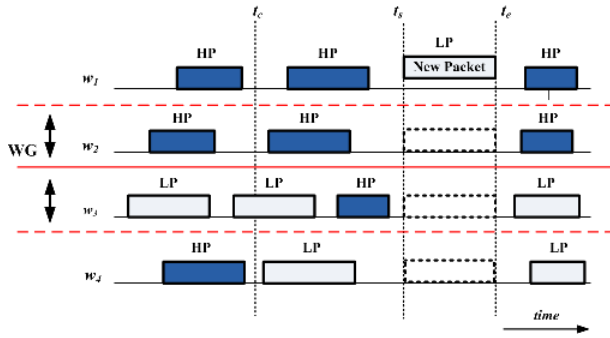


**FIGURE 4.** Dynamic Allocation of Wavelength Groups with Four Wavelengths.

The process is repeated whenever  $T(L_0, L_1)$  changes and a new  $w_{p0}$  is determined at current time. Consequently, wavelength partitioning changes over time with change in traffic load and reserved wavelengths for different service class traffic vary, employing the dynamic behavior of wavelength grouping. Moreover, when a HP optical packet is being scheduled on a wavelength on which a LP one has just been transmitted, the HP optical packet will be scheduled on latest available unscheduled time without preempting the LP optical packet. DWG adapt to fluctuating traffic loads by tracking the link status and then dynamically scheduling optical packets over most convenient wavelengths. DWG is rather more flexible approach than SWG, efficiently functional even when the share of HP traffic class is temporarily low. The dynamic allocation of available voids reduces blocking probability for both service classes traffic without dropping and preemption in rapidly varied traffic distribution. And therefore, contributes with improved bandwidth utilization for all traffic classes in an effort to provision good QoS with optimized network performance.

Pseudo-code for our proposed methodology is represented in Algorithm V.1 and V.2, which show the complete operation of DWG step by step.  $P_i$  represents any packet from  $L_\Psi$ ,  $Q_{disp}$  is dispatch buffer, and  $Q_{trans}$  is transmission queue of scheduler.

## V. SIMULATION SETUP

We conducted the simulation experimentations to validate and evaluate the performance of proposed DWG scheme using IBKSim [45] network simulator on two well-known network topologies: (i) the NSFNet with  $n_k = 16$  and  $l = 25$  (ii) the Cost239 with  $n_k = 11$  and  $l = 26$ , shown in Fig. 5 and Fig. 6 respectively. Each edge node acts as ingress switch and egress switch connected to a core switch. All connecting links are full duplex, include two distinct fibers with opposing directions. The lengths associated with the links in the topologies represent the physical distances between two nodes in kilometers. Note that these lengths were selected only for simulation purposes, these are not actual geographic distances of the networks.

### Algorithm V.1: PacketArrival( $P_i$ )

**if** Localpacket

```

    Insert packet into  $Q_{disp}$ 
     $P_i \leftarrow$  Front packet of  $Q_{disp}$ 
    Find channel using void-creating
    if Channel found
    then
        Reserve channel
        Remove  $P_i$  from  $Q_{disp}$ 
        then
             $P_i \leftarrow$  Forwarded to Scheduler  $Q_{trans}$ 
            Call ChannelAvailable( $t_e[P_i]$ )
        else
            Update statistics
             $P_i$  stays in  $Q_{disp}$ 

```

**else if** TransitPacket

```

    Find channel using void-creating
    if Channel found
    then
        Reserve channel
        then
            Call ChannelAvailable( $t_e[P_i]$ )
            Update statistics
        else
            Drop the packet  $P_i$ 
            Update statistics

```

### Algorithm V.2: ChannelAvailable()

```

 $Q_{disp}$  is not empty
 $P_i \leftarrow$  Front packet of  $Q_{disp}$ 
Find channel using void-creating
if ( $\Psi = 0$ )
    if Channel found
    then
        Pop  $P_i$  from  $Q_{disp}$ 
         $P_i \leftarrow$  Forwarded to Scheduler  $Q_{trans}$ 
         $L_\Psi \leftarrow$  Calculate load share  $T(L_0, L_1)$ 
         $\eta \leftarrow$  Calculate percentage of  $L_0$  from  $L_0/T(L_0, L_1)$ 
        then
             $w_{p0} \leftarrow$  Calculate no. of wavelengths required for  $L_0$  from  $\eta \times w_{ci}$ 
            Reserve channel
            Assign  $w_{p0} = (w_0, w_1, \dots, w_{p0-1})$  to  $L_0$ 
            Call ChannelAvailable( $t_e[P_i]$ )
            Update statistics
        else
             $P_i$  stays in  $Q_{disp}$ 

```

All of the nodes in simulation network are comparable to our baseline OPS model described in section III, where all the nodes have the same parameters and the same aggregation mechanisms. All switches are connected with packet sources

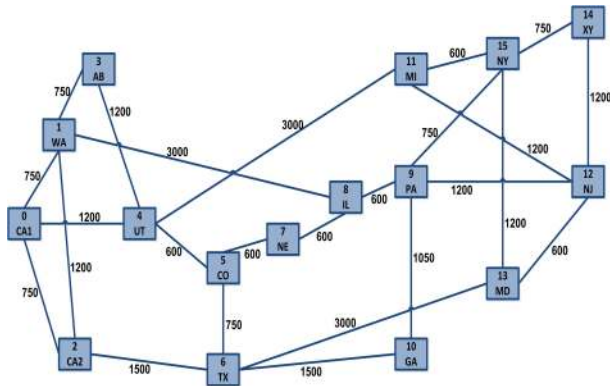


FIGURE 5. NSFNet topology with 16 nodes and 25 links.

which generate IP packets. For assembling of IP packets into optical packets, we chose threshold length value of 1 Mbit and threshold time value of  $100\mu s$  in assembly queues. The FCFS dispatch queues can buffer  $10^3$  optical packets at maximum. For the creation of external flows of packets, Poisson traffic model was assumed with exponentially distributed inter-arrival times and packet sizes with mean of 40 Kbps. It is nearly realistic because we get more smooth traffic in time-length hybrid assembly irrespective of its original characteristics.

The traffic is uniformly distributed between all intermediate node pairs. Processing time at each node for a control packet is  $10\mu s$  while propagation delay per kilometer for each packet is  $5\mu s/km$ . The routing decision is made on the basis of minimum number of hops, path with the least number of hops is taken as shortest path. The total simulation time includes 20 intervals and a transient or warm-up period and, 95% confidence interval is selected to find out the accuracy of output. In each simulation interval  $10^5$  packets are generated. We used the same two priority-class example, where class 1 is HP and class 0 is LP, and simulated these two priority classes with 16 wavelengths, each one of the capacity of 10 Gbps.

To realize the varying load share of each priority class in total load, we defined and simulated two scenarios of load variation on both NSFNet and Cost239 topologies.

### A. SCENARIO 1

In first scenario, we came up with a setting such that HP traffic share is started from 5% and gradually increased load of HP traffic by 5% in each step, up to maximum of 50% HP share in total load. In this way, LP traffic share is started from 95%, gradually decreased by 5% in each step up to minimum of 50% LP share in total load. At the end, we got a setting of 50% HP-50% LP, that is an equal-load scenario.

### B. SCENARIO 2

Second scenario is somehow opposite to the scenario 1. We started from equal-load, having 50% HP-50% LP load, reduced the share of HP traffic by 5% in each step of simulation until HP constituted 5% load of the total load. While LP traffic share is increased by the same factor 5%, up to

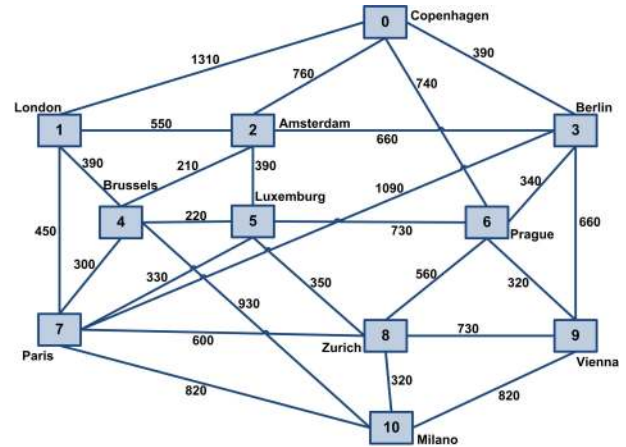


FIGURE 6. Cost239 topology with 11 nodes and 26 links.

the maximum of 95%. Thereby we got 5% HP-95% LP load setting.

## VI. RESULTS AND DISCUSSION

Impact of DWG is evaluated and QoS is measured in terms of average blocking probability over all network nodes and throughput. Mathematical equations for these metrics can be found in [44]. The proposed scheme is evaluated by comparing it with previously proposed SWG scheme. Fig. 7 to Fig. 14 show the results obtained for scenario 1 while Fig. 15 to Fig. 22 show the results for scenario 2 defined in previous section for both the topologies including blocking probability, throughput, and number of wavelengths.

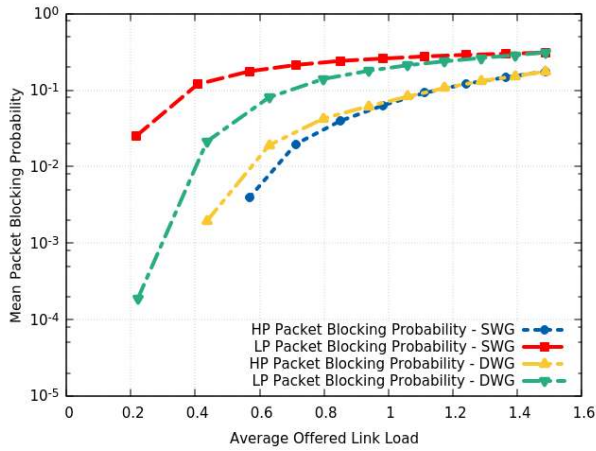
### A. RESULTS FOR SCENARIO 1

Fig. 7 shows relationships between mean packet blocking probability and average offered link load for NSFNet under SWG and DWG schemes. For SWG, wavelength grouping is set as 16-8 and load percentage of both HP and LP is taken exactly according to the scenario 1. Blocking probability is represented for each class separately which identifies that HP blocking is all the way less than the LP blocking. This means that HP packets will assist with more resources and undergo less dropping as compared to LP class because of limited wavelengths ensuring the QoS at every load point. The trait is found smooth and somehow curvy, showing considerable difference in blocking probability of both the HP class and LP class, and ensuring the QoS at every load point.

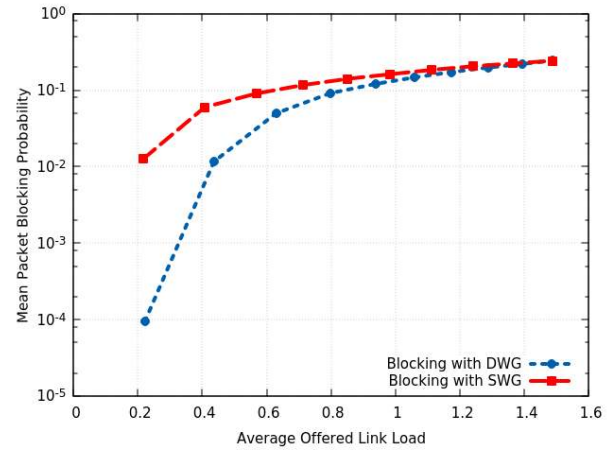
The QoS blocking with our proposed scheme DWG for NSFNet in the function of normalized link load is achieved over the same load variation for HP and LP as it was in SWG (defined in scenario 1 in section V), but this time wavelengths for both classes are not fixed. DWG determines the wavelengths for packets of each class according to their share in total load. The trend is more smooth and curvier in DWG, absolutely no blocking till 0.4 load. Difference in blocking of HP and LP shows that DWG maintains QoS at every point of load.

Fig. 8 demonstrates the QoS blocking probability for our second topology i.e., Cost239 under SWG and DWG.





**FIGURE 7.** Mean QoS packet blocking probability in NSFNet with SWG and DWG (scenario 1).



**FIGURE 9.** Comparison of total packet blocking probability of SWG and DWG in NSFNet (scenario 1).

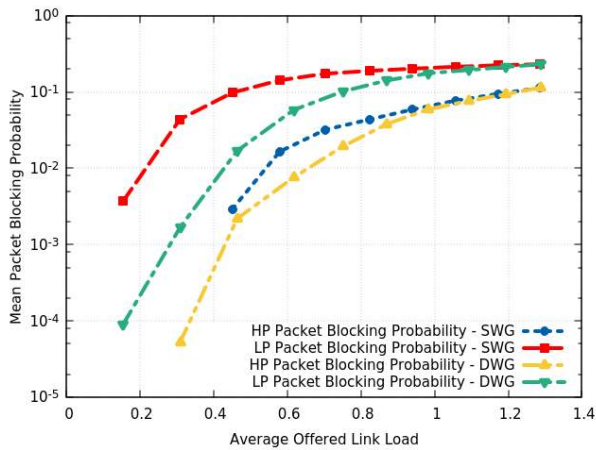


**FIGURE 8.** Mean QoS packet blocking probability in Cost239 with SWG and DWG (scenario 1).

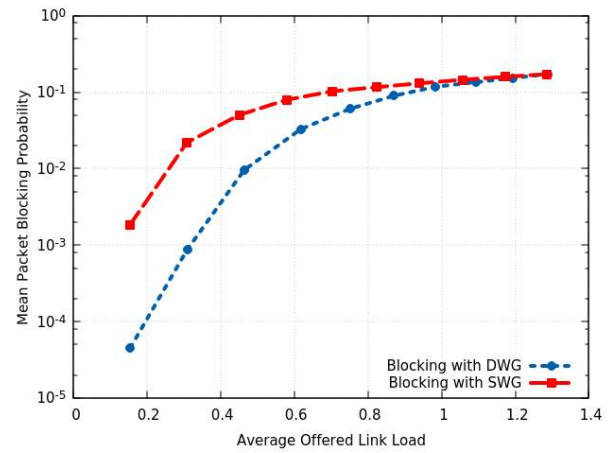


**FIGURE 10.** Comparison of total packet blocking probability of SWG and DWG in Cost239 (scenario 1).

Here, outcomes are more or less same as NSFNet but statistical values of blocking are different due to different layout of Cost239 (shorter links and higher connectivity). However, it is observed that characteristics for HP and LP are in some way equidistant in DWG. We noted that the absolute QoS property of wavelength grouping stated earlier is sustained at every load point in both SWG and DWG for both the topologies, giving the idea that employment of proposed scheme is independent of network topology.

Fig. 9 compares our proposed DWG with SWG for NSFNet under scenario 1. Analysis shows that at starting, when HP load share is less (5% HP) and LP load share is at its maximum (95% LP), DWG gives the optimized performance as compared to SWG. There is a huge difference in blocking at 0.2 load, roughly 21% improvement. Because at this stage HP class is facilitated with only 1 or 2 wavelengths and LP class is supported with maximum resources which was limited in SWG 16-8 wavelength grouping.

However, rise in DWG graph line is more dramatic, when HP share is increased gradually, blocking difference moderately get reduced and finally SWG and DWG become identical at equal-load scenario i.e. (50% HP – 50% LP)

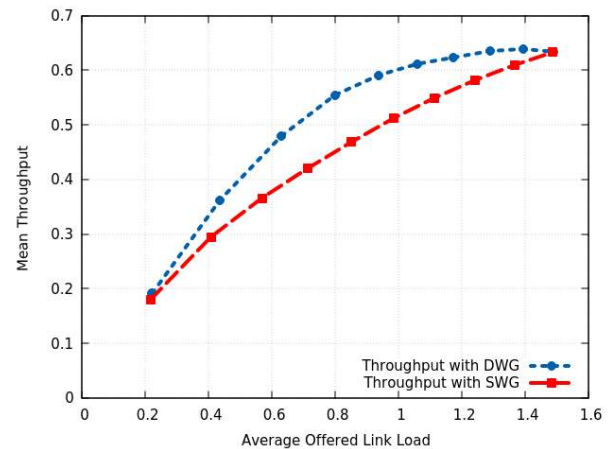


**FIGURE 11.** Throughput Comparison of DWG and SWG for NSFNet (scenario 1).

because at this point, DWG resulting wavelength grouping is also 16-8.

When it comes to Cost239, all the attributes can be seen more clearly (Fig. 10). Outcomes possess quite same trend as NSFNet but more even due to the reason mentioned earlier. Like in NSFNet, DWG works in fluctuating traffic load of HP

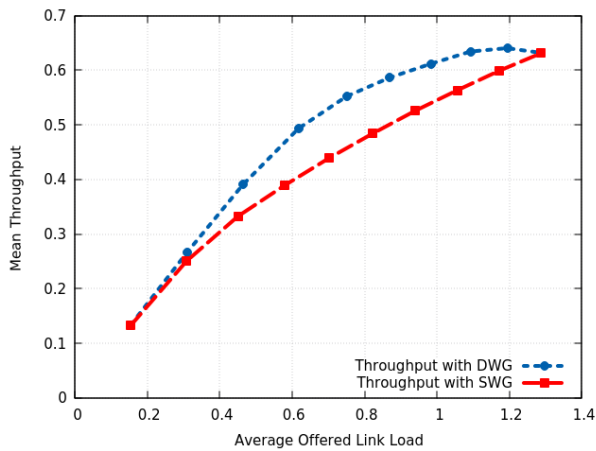


**FIGURE 12.** Throughput Comparison of DWG and SWG for Cost239 (scenario 1).

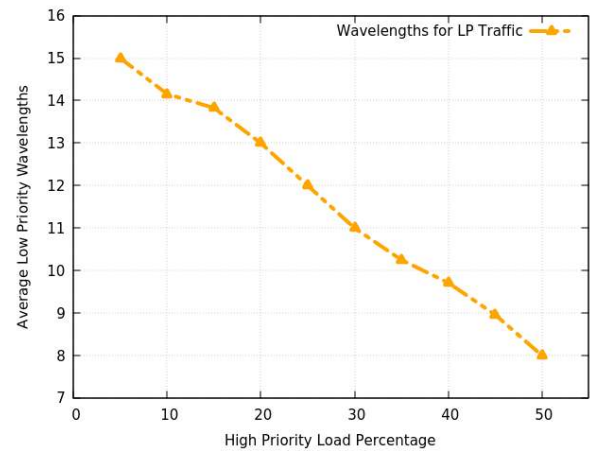


**FIGURE 14.** Average wavelengths for low priority traffic under DWG in Cost239 (scenario 1).

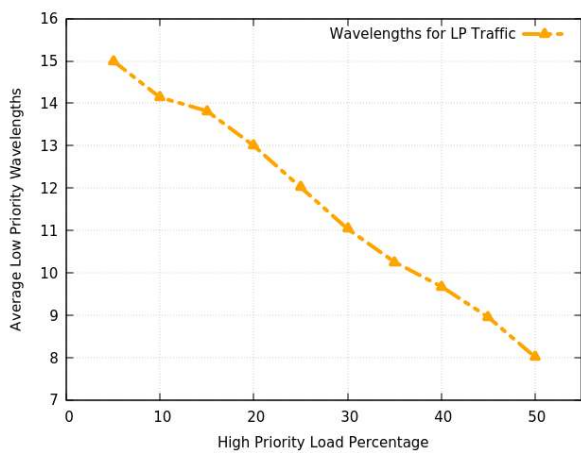


**FIGURE 13.** Average wavelengths for low priority traffic under DWG in NSFNet (scenario 1).

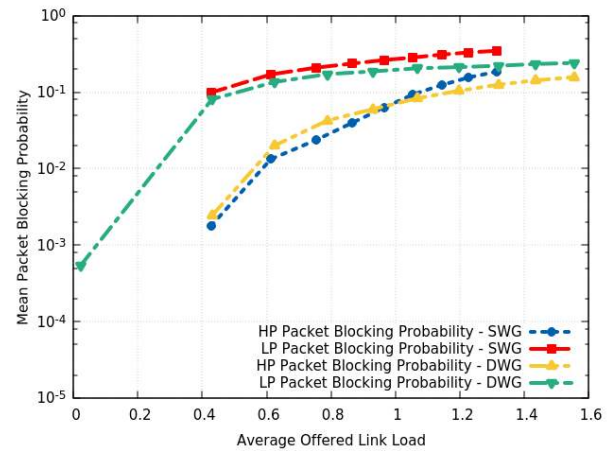


**FIGURE 15.** Mean QoS packet blocking probability in NSFNet with SWG and DWG (scenario 2).

and LP class and gives overall improved performance than SWG. Fig. 9 and Fig. 10 validate that DWG is applicable regardless the network topology. Besides, both the conditions of DWG are fulfilled here; we get improved mean blocking probability in DWG with QoS in fluctuating load scenario. Overall packet blocking is reduced by 21% and at the same time QoS provisioning is maintained at every load share of scenario 1 of both HP and LP class.

Fig. 11 and Fig. 12 indicate network throughput at different load calculated at different time points during simulation of scenario 1 for NSFNet and Cost239 topologies respectively. Throughput against SWG is rather linear, equally space, and fast-paced, increasing rapidly with increase in load despite of individual load of HP and LP class. Both the topologies depict same throughput leaning but there is statistical difference which can be realized from Fig. 11 and Fig. 12. In proposed DWG, the graph shows very interesting tendency, increases linear and rapidly but curvier than SWG. At start, SWG and DWG gives same throughput but with time progression and load increment, DWG throughput increases and exhibits maximum difference at 0.8 load having 25% HP and 75% LP traffic. However, at equal-load scenario, DWG throughput

acquires the same value as of SWG. Concisely, we get better mean throughput at variable load scenarios when HP class load is varied from 5% to 49%, perceive the idea that DWG is far better technique than SWG.

To understand the wavelength distribution for each priority traffic under DWG, Fig. 13 (NSFNet) and Fig. 14 (Cost239) illustrate the number of wavelengths assigned to LP class in result of varying percentage of HP class from 5% to 50% of scenario 1. Wavelength grouping is done on the basis of load percentages of both the classes. Initially when HP is 5% and LP is 95%, LP is entertained with 15 wavelengths, yielding 16-15 wavelength grouping. Wavelengths for LP is decreased almost linearly with increase in HP share and attains the grouping of 16-8 at 50% HP and 50% LP.

## B. RESULTS FOR SCENARIO 2

Fig. 15 illustrates mean blocking probability of packets in the function of average offered link load for NSFNet under SWG and DWG schemes. Here wavelength grouping is set as 16-8, same as scenario 1 of SWG, but scenario 2 is used for determining the load percentages of both HP and LP classes in total load. This figure clearly depicts that HP blocking is

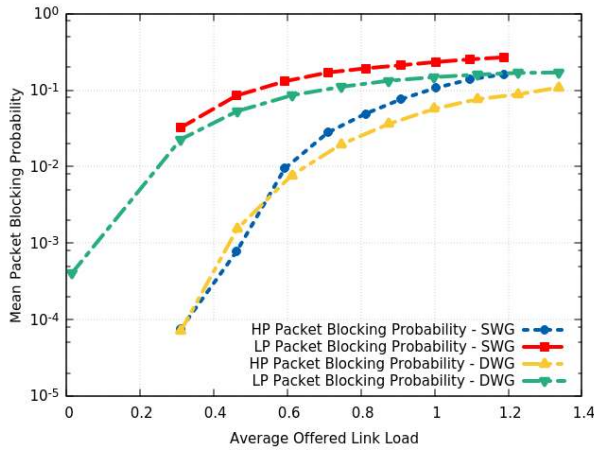


**FIGURE 16.** Mean QoS packet blocking probability in Cost239 with SWG and DWG (scenario 2).

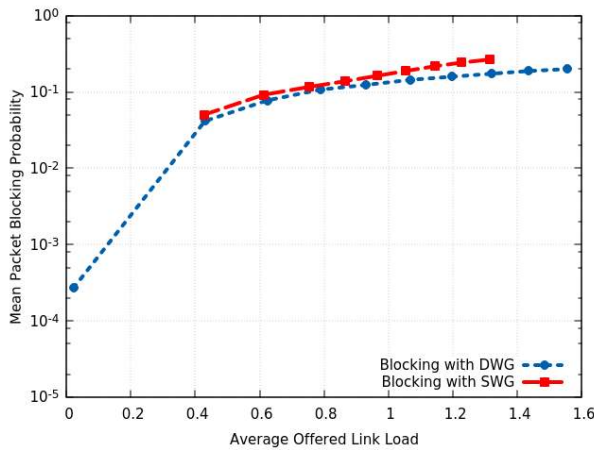


**FIGURE 17.** Comparison of total packet blocking probability of SWG and DWG in NSFNet (scenario 2).

less than the LP blocking. Due to the limited wavelengths, SWG blocking for LP class is relatively high and has less margin between its starting and ending point. The behavior of HP blocking is more engaging, giving the idea that resources for HP class are fairly utilized. Though, this difference in blocking probability of both the HP class and LP class and reveals that QoS is ensured at every load point.

In regard to the QoS blocking of our proposed scheme DWG for NSFNet in terms of average offered link load, percentage of load for HP and LP class is obtained from scenario 2 and DWG is applied in order to determine the wavelengths for both classes. In case of DWG for LP class, we see blocking right after start of the simulation i.e. 50% HP and 50% LP share, while for HP class there is no blocking till 0.4 load. Difference in blocking of HP and LP shows that DWG maintains QoS at every point of load.

Considering the Cost239 topology, the QoS blocking under SWG and DWG is demonstrated collectively in Fig. 16, while keeping the simulation parameters, load variation scenario, and evaluation criterion same as NSFNet. Cost239 topology always gives more satisfactory results, as it can be seen in figure that LP blocking is almost as same as NSFNet but

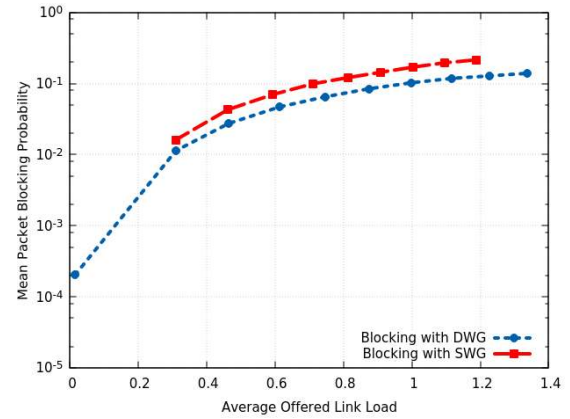


**FIGURE 18.** Comparison of total packet blocking probability of SWG and DWG in Cost239 (scenario 2).

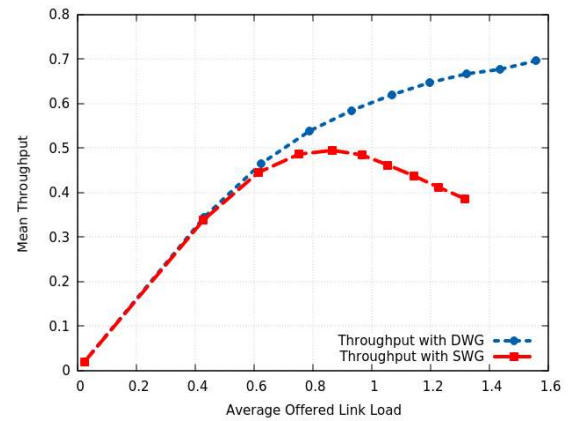


**FIGURE 19.** Throughput Comparison of DWG and SWG for NSFNet in scenario 2.

HP blocking show a complete curve. Here QoS difference can be observed more precisely at load 0.2, the difference is highest at beginning in equal-load setting and gradually reduced with decrease in HP load share. However, this difference is carried till the end, lines do not meet at the end (guarantees QoS). Like scenario 1, absolute QoS property of wavelength grouping is kept at every load point in both SWG and DWG techniques for both NSFNet and Cost239 topologies. Therefore, DWG is operative in varying traffic loads no matter HP class load is rising or falling.

Comparison of our proposed DWG with SWG for NSFNet topology under load variation of scenario 2 is shown in Fig. 17. Here DWG offers optimized performance because it operates at every value of load when HP varies from 50% to 5% and gives some value of blocking, but SWG effects only a limited range of the load (0.4 to 1.25). Results show improvement in DWG blocking at every point of the graph. However, rise in DWG graph line is more rapid than SWG. Although HP share is decreased gradually but this decrease does not affect the blocking difference even at the end. Here, if we compare the results of scenario 1 with scenario 2 under same conditions, it can be concluded that DWG is highly functional when HP load variation is between 50% to 5%.

Trends can be realized more accurately while considering the Cost239, in Fig. 18. Outcome characteristics are like

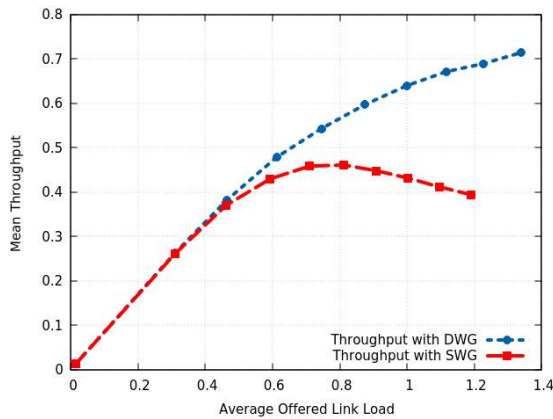


**FIGURE 20.** Throughput Comparison of DWG and SWG for Cost239 in scenario 2.

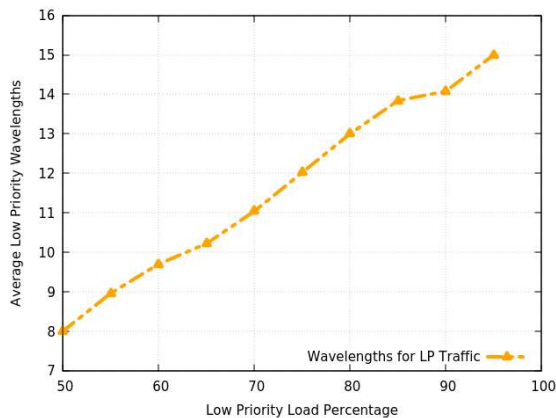


**FIGURE 21.** Average wavelengths for low priority traffic under DWG in NSFNet in scenario 2.

NSFNet but more smooth, curvier, and equidistant at all points of graph. DWG works in rapidly changing traffic load of HP and LP class and gives overall enhanced performance than SWG. If we have a collective look on all graphs, we must say that DWG gives improved mean blocking probability with maintained QoS in fluctuating load scenarios. Total packet blocking is reduced significantly, and this effect is more obvious when we start from equal-load scenario and decrement of share of HP class i.e., 50% HP to 5% HP (scenario 2).

Fig. 19 and Fig. 20 show the comparison between network throughputs achieved at different load points under SWG and DWG of scenario 2 for NSFNet and Cost239 topology separately. Both the topologies describe same throughput trend but there is statistical difference which can be realized from Fig. 19 and Fig. 20. Throughput of the scenario 2 exhibits an unexpected and extraordinary behavior as compared to scenario 1 because of the load settings. Throughput concerning SWG is rather linear in the beginning and increases rapidly till 0.8 load (having 25% HP and 75% LP) but after that, throughput starts decreasing functionally until the HP load reaches at 5% of the total load which significantly reduces the gain of SWG. On the other hand, in proposed DWG, the graph shows remarkable increment in mean throughput at

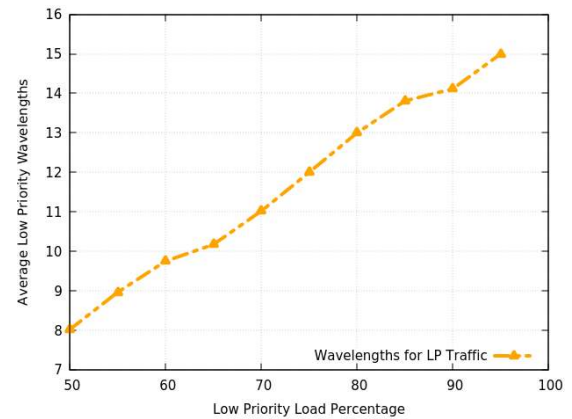


**FIGURE 22.** Average wavelengths for low priority traffic under DWG in Cost239 in scenario 2.

every load despite the percentage of individual load of HP and LP class. Although at equal-load point and until the 0.45 value of load (40% HP and 60% LP) we get same throughput under both SWG and DWG but after 0.5 load, DWG throughput increases at fast pace and SWG undergo decrease in throughput resulting roughly 30% difference when reaches at 5% HP and 95% LP traffic.

Consequently, proposed DWG scheme improves the mean throughput by 30% at variable load scenarios when HP class load is varied from 50% to 5%.

Fig. 21 and Fig. 22 give the number of wavelengths assigned to LP class in result of varying percentage of LP class from 50% to 95% of the scenario 2 for NSFNet and Cost239. Like scenario 1 wavelength grouping is done according to the share of each class in total load. But here, trend is opposite because we start from equal-load (50% HP and 50% LP), so we come up with 16-8 wavelength distribution. Gradual increase in LP class leads the increase in LP wavelength and we achieve the grouping of 16-15 at 5% HP and 95% LP.

Statistical and graphical comparison of both the techniques show a significant improvement in average QoS blocking as well as total blocking. A gain in network throughput is also achieved which makes DWG more favorable. From the results, it is evident that proposed DWG is much more flexible approach and so right choice among the wavelength reservation schemes. DWG utilizes the available network resources efficiently and does not require additional hardware like other static WAR and AWs schemes. It enhances the network performance in terms of above-mentioned parameters and so a QoS-enabled competent OPS backbone network is realized with efficient utilization of wavelength resources and optimized performance.

## VII. CONCLUSION

This paper proposed and analyzed an advanced technique DWG for absolute QoS in an OPS, which makes dynamic and most appropriate partitions of available wavelength resources and allocate them to traffic of each class of service in rapidly varying traffic loads by tracking the current link load status.



The wavelength grouping changes over time with change in load share of each class, and results in efficient utilization of wavelength resources at each link. We described a baseline OPS model to express the expected performance, and then briefly examined the proposed technique over various QoS metrics to evaluate its performance and effectiveness. A number of possible simulation scenarios are evaluated to understand the effect of DWG on blocking probability in fluctuating traffic loads of different classes. The simulations show that DWG outperforms the previous SWG and provides improved blocking with guarantee of QoS provisioning, by giving the optimal partitioning of wavelengths on demand among classes of high and low priority traffic in varying traffic load scenarios. The graphical results show improvement in mean blocking probability of packets and network throughput by a total of about 21% and 30% respectively. The results are obtained with assumption of just two service classes, we believe that DWG is equally efficient even when the number of priority classes increases, and load fluctuations get relatively more complicated. In future, we aimed to analyze DWG with more functions like PLR, PDV, bit error rate and response time. Also, design a framework provisioning of resources in more adverse load situations at edge OPS switches with assurance of same impact on these factors.

## CONFLICT OF INTEREST

We herein notify that authors have no conflict of interest.

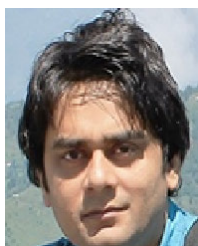
## REFERENCES

- [1] A. G. Rahbar, *Quality of Service in Optical Packet Switched Networks*. Hoboken, NJ, USA: Wiley, 2015.
- [2] K. Kitayama, "Optical packet switching: Myth, fact, and promise," in *Proc. OptoElectron. Commun. Conf. (OECC)*, Niigata, Japan, 2016, pp. 1–2.
- [3] J. P. Jue and V. M. Vokkarane, *Optical Burst Switched Networks*. New York, NY, USA: Springer, 2006.
- [4] H. Øverby, "Traffic modelling of asynchronous bufferless optical packet switched networks," *Comput. Commun.*, vol. 30, no. 6, pp. 1229–1243, Mar. 2007.
- [5] S. Gunreben, "An optical burst reordering model for time-based and random selection assembly strategies," *Perform. Eval.*, vol. 68, no. 3, pp. 237–255, Mar. 2011.
- [6] T. Holyński and M. F. Hayat, "Analysis of OBS burst assembly queue with renewal input," *Adv. Electron. Telecommun.*, vol. 2, no. 3, pp. 23–30, 2011.
- [7] M. F. Hayat, T. Holyński, and F. Z. Khan, "Restricted intermediate buffering in OBS networks with combined nodes," in *Proc. 39th Int. Conf. Telecommun. Signal Process. (TSP)*, Vienna, Austria, Jun. 2016, p. 6.
- [8] R. S. Barpanda, A. K. Turuk, and B. Sahoo, "QoS aware routing and wavelength allocation in optical burst switching networks using differential evolution optimization," *Digit. Commun. Netw.*, vol. 4, no. 1, pp. 3–12, Feb. 2018.
- [9] M. Imran and K. Aziz, "Quality of service in hybrid optical switching," in *Proc. 12th Int. Conf. Frontiers Inf. Technol.*, Islamabad, Pakistan, Dec. 2014, pp. 7–10.
- [10] H. Meyer, J. C. Sancho, M. Mrdakovic, W. Miao, and N. Calabretta, "Optical packet switching in HPC. An analysis of applications performance," *Future Gener. Comput. Syst.*, vol. 82, pp. 606–616, May 2018.
- [11] P. Andreades, K. Clark, P. M. Watts, and G. Zervas, "Experimental demonstration of an ultra-low latency control plane for optical packet switching in data center networks," *Opt. Switching Netw.*, vol. 32, pp. 51–60, Apr. 2019.
- [12] F. Kharroubi, L. Chen, and J. Yu, "Approaches and controllers to solving the contention problem for packet switching networks: A survey," in *Internet of Things* (Communications in Computer and Information Science), vol. 312. Berlin, Germany: Springer, 2012, pp. 172–182.
- [13] C. Ware, W. Samoud, P. Gravey, and M. Lourdiane, "Recent advances in optical and hybrid packet switching," in *Proc. 18th Int. Conf. Transparent Opt. Netw. (ICTON)*, Jul. 2016, pp. 1–4.
- [14] F. Z. Khan, M. F. Hayat, T. Holyński, and M. J. Khan, "Towards dynamic wavelength grouping for QoS in optical burst-switched networks," in *Proc. 40th Int. Conf. Telecommun. Signal Process. (TSP)*, Jul. 2017, pp. 79–85.
- [15] W. Wei, Q. Zeng, Y. Ouyang, and D. Lomone, "Differentiated integrated QoS control in the optical Internet," *IEEE Commun. Mag.*, vol. 42, no. 11, pp. S27–S34, Nov. 2004.
- [16] Q. Zhang, V. M. Vokkarane, J. P. Jue, and B. Chen, "Absolute QoS differentiation in optical burst-switched networks," *IEEE J. Sel. Areas Commun.*, vol. 22, no. 9, pp. 1781–1795, Nov. 2004.
- [17] A. G. P. Rahbar and O. W. W. Yang, "Contention avoidance and resolution schemes in bufferless all-optical packet-switched networks: A survey," *IEEE Commun. Surveys Tuts.*, vol. 10, no. 4, pp. 94–107, 4th Quart., 2008.
- [18] A. M. Kaczmarek, "Methods of analyses, providing and differentiation schemes quality of service in optical packet/burst switched networks," M.S. thesis, Dept. Interact. Syst. Des., School Eng., Blekinge Inst. Technol., Karlskrona, Sweden, 2008.
- [19] A. Kavitha, "Performance of optical networks: A short survey," *Int. J. Eng. Sci. Technol.*, vol. 4, no. 2, pp. 600–605, 2012.
- [20] F. Xue, Z. Pan, Y. Bansal, J. Cao, M. Jeon, K. Okamoto, S. Kamei, V. Akella, and S. J. B. Yoo, "End-to-end contention resolution schemes for an optical packet switching network with enhanced edge routers," *J. Lightw. Technol.*, vol. 21, no. 11, pp. 2595–2604, Nov. 2003.
- [21] R. Nejibati, G. Zervas, D. Simeonidou, M. J. O'Mahony, and D. Klondis, "The 'OPORON' project: Demonstration of a fully functional end-to-end asynchronous optical packet-switched network," *J. Lightw. Technol.*, vol. 25, no. 11, pp. 3495–3510, Nov. 2007.
- [22] A. G. Rahbar and O. Yang, "Fiber-channel trade-off for reducing collisions in slotted single-hop optical packet-switched networks," *J. Opt. Netw.*, vol. 6, no. 7, pp. 897–912, 2007.
- [23] S. Bjørnstad and H. Øverby, "Quality of service differentiation in optical packet/burst switching: A performance and reliability perspective," in *Proc. IEEE 7th Int. Conf. Transparent Opt. Netw.*, vol. 1, Jul. 2005, pp. 85–90.
- [24] M. Asghari and A. G. Rahbar, "Contention avoidance in bufferless slotted optical packet switched networks with egress switch coordination," *Opt. Switching Netw.*, vol. 18, pp. 104–119, Nov. 2015.
- [25] M. Asghari and A. G. Rahbar, "Contentionless transmission in bufferless slotted optical packet switched networks," *Opt. Fiber Technol.*, vol. 30, pp. 134–146, Jul. 2016.
- [26] A. G. Rahbar, "PTES: A new packet transmission technique in bufferless slotted OPS networks," *J. Opt. Commun. Netw.*, vol. 4, no. 6, pp. 490–502, Jun. 2012.
- [27] K. Kralevska, H. Øverby, and D. Gligoroski, "Coded packet transport for optical packet/burst switched networks," in *Proc. IEEE Global Commun. Conf. (GLOBECOM)*, Dec. 2015, pp. 1–6.
- [28] H. Øverby and N. Stol, "QoS differentiation in asynchronous bufferless optical packet switched networks," *Wireless Netw.*, vol. 12, no. 3, pp. 383–394, Jun. 2006.
- [29] Z. Lu, D. K. Hunter, and I. D. Henning, "Contention resolution scheme for slotted optical packet switched networks," in *Proc. IEEE Conf. Opt. Netw. Design Modeling (IEEE ONDM)*, Feb. 2005, pp. 227–234.
- [30] S. Haeri and L. Trajković, "Intelligent deflection routing in bufferless networks," *IEEE Trans. Cybern.*, vol. 45, no. 2, pp. 316–327, Feb. 2015.
- [31] T. Khattab, A. Mohamed, A. Kaheel, and H. Alnuweiri, "Optical packet switching with packet aggregation," in *Proc. Int. Conf. Softw., Telecommun., Comput. Netw. (SOFTCOM)*, 2002, pp. 1–6.
- [32] M. A. Yazici and N. Akar, "Performance modeling of QoS differentiation in optical packet switching via FDL access limitation," *Photonic Netw. Commun.*, vol. 34, pp. 344–355, May 2017.
- [33] A. G. P. Rahbar and O. W. W. Yang, "Distribution-based bandwidth access scheme in slotted all-optical packet-switched networks," *Comput. Netw.*, vol. 53, no. 5, pp. 744–758, Apr. 2009.
- [34] S. Bjørnstad et al., "Optical burst and packet switching: Node and network design, contention resolution and quality of service," in *Proc. 7th Int. Conf. Telecommun. (ConTEL)*, vol. 2, 2003, pp. 775–778.
- [35] H. Øverby, "An adaptive service differentiation algorithm for optical packet switched networks," in *Proc. 5th Int. Conf. Transparent Opt. Netw.*, vol. 1, 2003, pp. 158–161.
- [36] D. H. Hailu, G. G. Lema, E. A. Yekun, and S. H. Kebede, "Unified study of quality of service (QoS) in OPS/OBS networks," *Opt. Fiber Technol.*, vol. 36, pp. 394–402, Jul. 2017.

- [37] H. Øverby, "How the packet length distribution influences the packet loss rate in an optical packet switch," in *Proc. Adv. Int. Conf. Telecommun. Int. Conf. Internet Web Appl. Services (AICT-ICIW)*, 2006, p. 46.
- [38] M. Nord and H. Øverby, "Packet loss rate and jitter differentiating quality-of-service schemes for asynchronous optical packet switches," *J. Opt. Netw.*, vol. 3, no. 12, pp. 866–881, 2004.
- [39] Q. Zhang, V. M. Vokkarane, B. Chen, and J. P. Jue, "Early drop and wavelength grouping schemes for providing absolute QoS differentiation in optical burst-switched networks," in *Proc. Global Telecommun. Conf. (GLOBECOM)*, vol. 5, 2003, pp. 2694–2698.
- [40] Z. Lu and D. K. Hunter, "Optical packet contention resolution through edge smoothing into decomposed subflows," *J. Opt. Commun. Netw.*, vol. 1, no. 7, pp. 622–635, Dec. 2009.
- [41] C. Raffaelli and P. Zaffoni, "Packet assembly at optical packet network access and its effects on TCP performance," in *Proc. Workshop High Perform. Switching Routing (HPSR)*, 2003, pp. 141–146.
- [42] M. Nord, S. Bjørnstad, and C. M. Gauger, "OPS or OBS in the core network?" in *Proc. 7th IFIP Workshop Conf. Opt. Netw. Design Modeling*, Budapest, Hungary, 2003, pp. 179–198.
- [43] A. G. P. Rahbar and O. Yang, "Prioritized retransmission in slotted all-optical packet-switched networks," *J. Opt. Netw.*, vol. 5, no. 12, pp. 1056–1070, 2006.
- [44] F. Z. Khan, "Analysis of optical burst switched networks with edge-core joint nodes," Ph.D. dissertation, Inst. Telecommun., Vienna Univ. Technol., Vienna, Austria, 2012. Available: [Online]. Available: <http://fms.uettaxila.edu.pk/downloads/FZKThesis.pdf>
- [45] L. Wallentin, M. Happenhofer, C. Egger, and J. Fabini, "XML meets simulation: Concepts and architecture of the IBKSim network simulator," *Simul. Notes Eur.*, vol. 20, no. 1, pp. 16–20, Apr. 2010.



**HAFSA BIBI** received the B.S. degree in telecommunication and networking from COMSATS University Islamabad, Pakistan, in 2016, and the M.S. degree in computer science from the University of Engineering and Technology Taxila, Pakistan, in 2019. Her major research interests include optical networks specifically optical packet switched networks and wavelength division multiplexing networks. Her research efforts are about bringing novelty in Optical Networks in terms of Quality of Service.



**FARRUKH ZEESHAN KHAN** received the master's degree in computer science from the Islamia University Bahawalpur, Pakistan, in 2002, and the Ph.D. degree in telecommunications from the Institute of Telecommunications, Vienna University of Technology, Vienna, Austria, in 2012. During Ph.D. studies, he worked on optical burst switched network. He is currently working as an Assistant Professor with the Computer Science Department, University of Engineering and Technology, Taxila, Pakistan. His research interests include the Internet of Things, mobile adhoc networks, and next generation all-optical networks.



**MUNEER AHMAD** (Member, IEEE) received the Ph.D. in computer science from the Universiti Teknologi PETRONAS, Malaysia, in 2014. He has 18 years of teaching, research, and administrative experience internationally. He successfully completed several funded research projects. He has authored numerous research papers in refereed research journals, international conferences, and books. His research interests include data science, big data analysis, machine learning, bioinformatics, and medical informatics.



ardous environment. Her major research interest includes the Internet of Things.

**ANUM NASEEM** received the M.S. (CS) degree from the University of Engineering and Technology, Taxila, Pakistan, in 2018. She is currently a Lecturer with the Computer Science Department, University of Lahore, Islamabad Campus, Pakistan. She has experienced in network programming and network operating system (Linux). She is working on the performance evaluation of the IoT. She worked on a project named autonomous robot for strategic surveillance in hazardous environment. Her major research interest includes the Internet of Things.



**TOMASZ HOLYNSKI** received the M.Sc. degree, in 2009. He studied telecommunications and computer science jointly at the Technical University of Lodz, Poland, and at the Vienna University of Technology (VUT), Austria. He was a Project- and Research Assistant with the Institute of Broadband Communications and the Institute of Telecommunications, VUT. His research concerned analyses of error-correction protocols, congestion resolution in all-optical networks, and clustering algorithms for sensor networks. He is currently with the Institute of Statistics and Mathematical Methods in Economics, VUT, realizing his doctoral programme. He works on statistical methods based on Fourier transforms including robust estimation, goodness-of-fit and various semiparametric tests. His research interests include statistical learning, simulation, and network modeling. His master thesis on queueing theoretical modeling was distinguished by the Austrian Electrotechnical Association with the GIT-Award.



**KELVIN J. A. OOI** received the B.Eng. (Hons.) and Ph.D. degrees from Nanyang Technological University (NTU), Singapore, in 2010 and 2014, respectively. From 2014 to 2018, he was a Post-doctoral Research Fellow with the SUTD-MIT International Design Center (IDC) and the Lee Kuan Yew Center for Innovative Cities (LKCYIC), Singapore University of Technology and Design (SUTD). He is currently an Assistant Professor with the Department of Physics, Xiamen University Malaysia (XMUM). He has authored over 60 international journal and conference papers, which include top-tier journals like *Nature Communications* and *ACS Photonics*. His current research interests include span interdisciplinary domains, which include low-dimensional optical physics, electromagnetic neurophysics, urban traffic physics, and sustainable systems and architecture. He was a recipient of several national and university research grants, including one awarded by the Ministry of Higher Education Malaysia under its Fundamental Research Grant Scheme (FRGS).



**JAVED AHMED MAHAR** received the M.Sc. degree in computer science from Shah Abdul Latif University, Khairpur, Pakistan, in 1996, the M.S. degree in computer science from the Karachi Institute of Economics and Technology (PAF-KIET), Karachi, Pakistan, in 2007, and the Ph.D. degree from Hamdard University, Karachi, in 2012. He is currently a Professor with the Department of Computer Science, Shah Abdul Latif University. He has got more than 22 years of teaching experience. He has published several articles in national and international journals and peer-reviewed conference proceedings. His research interests include natural language processing, speech and image processing, big data analytics, software engineering, and programming paradigms.

...